

## Supplementary Information

# Multiscale Crack Initiators Promoted Super-Low Ice Adhesion Surfaces

*Zhiwei He<sup>†</sup>, Senbo Xiao<sup>†</sup>, Huajian Gao<sup>‡</sup>, Jianying He<sup>†</sup> and Zhiliang Zhang<sup>\*†</sup>*

<sup>†</sup> NTNU Nanomechanical Lab, Department of Structural Engineering, Norwegian University of Science and Technology (NTNU), Trondheim 7491, Norway

<sup>‡</sup> Division of Engineering, Brown University, Providence, RI 02912, USA

Correspondence and requests for materials should be addressed to Z.Z. (email: zhiliang.zhang@ntnu.no)

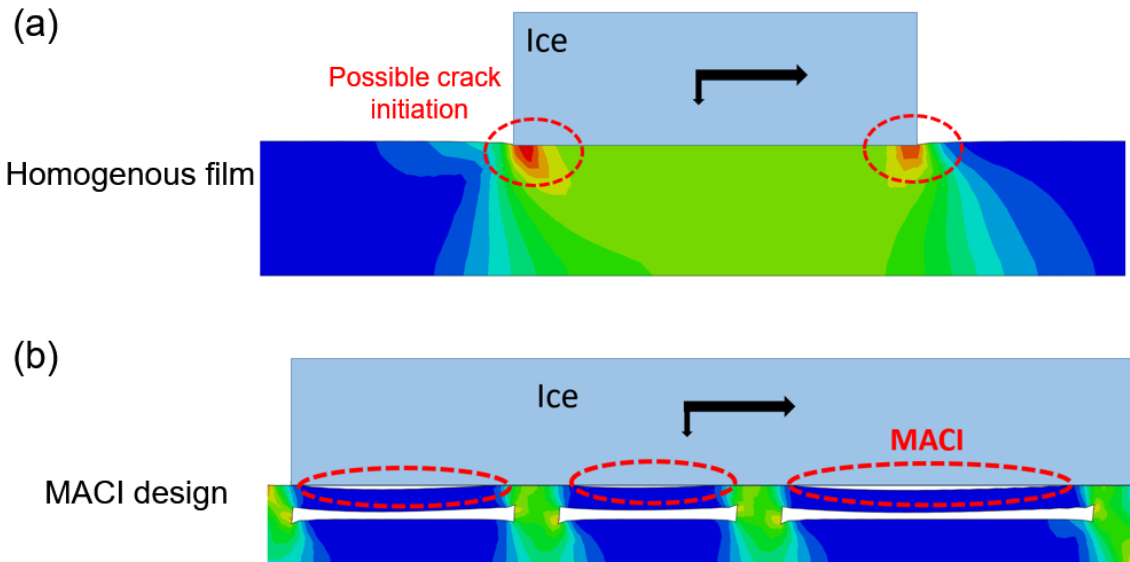


**Fig. S1.** 2D plane strain finite element analyses using ABAQUS to illustrate the MACI mechanism, (a) ice adhesion test on a homogenous film; and (b) ice adhesion test on the proposed film with substructures. The black arrows resemble the applied forces. In (a) stress concentration at the corners of the ice cube can be expected, which could possibly initiate cracks. In contrast, the film with substructures introduced in this study shown in (b), will generate macroscopic cracks along the complete length of the interface. Here the MACI mechanism is obvious as indicated by macro-sized cracks.

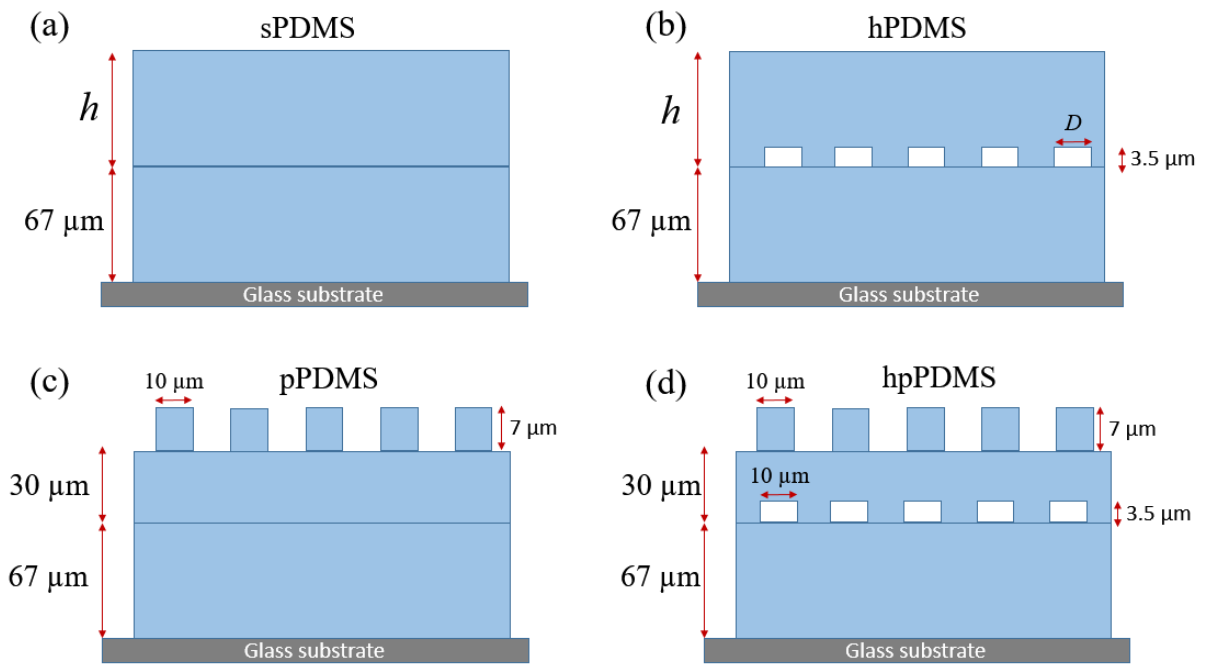


**Fig. S2. Schematic overview of (a) sPDMS, (b) hPDMS, (c) pPDMS and (d) hpPDMS.** The layer thickness  $h$  of (a) sPDMS and (b) hPDMS alters from 30, 36, 67 to 115  $\mu\text{m}$ . The diameter  $D$  of internal holes for (b) hPDMS alters from 10  $\mu\text{m}$ , 100  $\mu\text{m}$ , 1 mm to 2 mm.

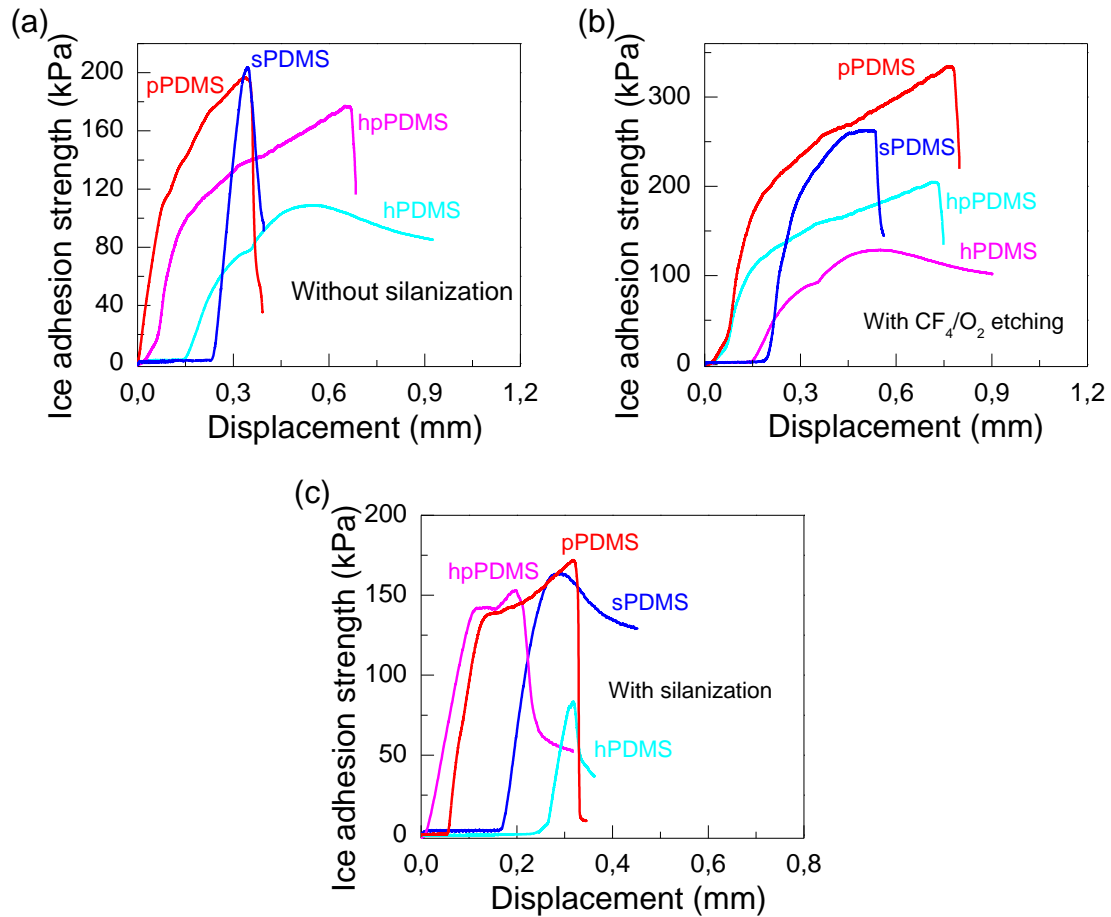


**Fig. S3.** Ice adhesion strength of PDMS thin films at -18 °C against displacement. (a) As-prepared; (b) CF<sub>4</sub>/O<sub>2</sub> etched; and (c) silanized. The single layer thickness is 30 μm, the diameter of internal holes and outer pillars is 10 μm, the curing temperature is 65 °C, and the weight ratio is 10:1. To realize the design of PDMS with sub-structures as suggested by finite element analysis (**Fig. S1**), a 67 μm thick thin film of PDMS was coated on glass before preparing targeted PDMS thin films.

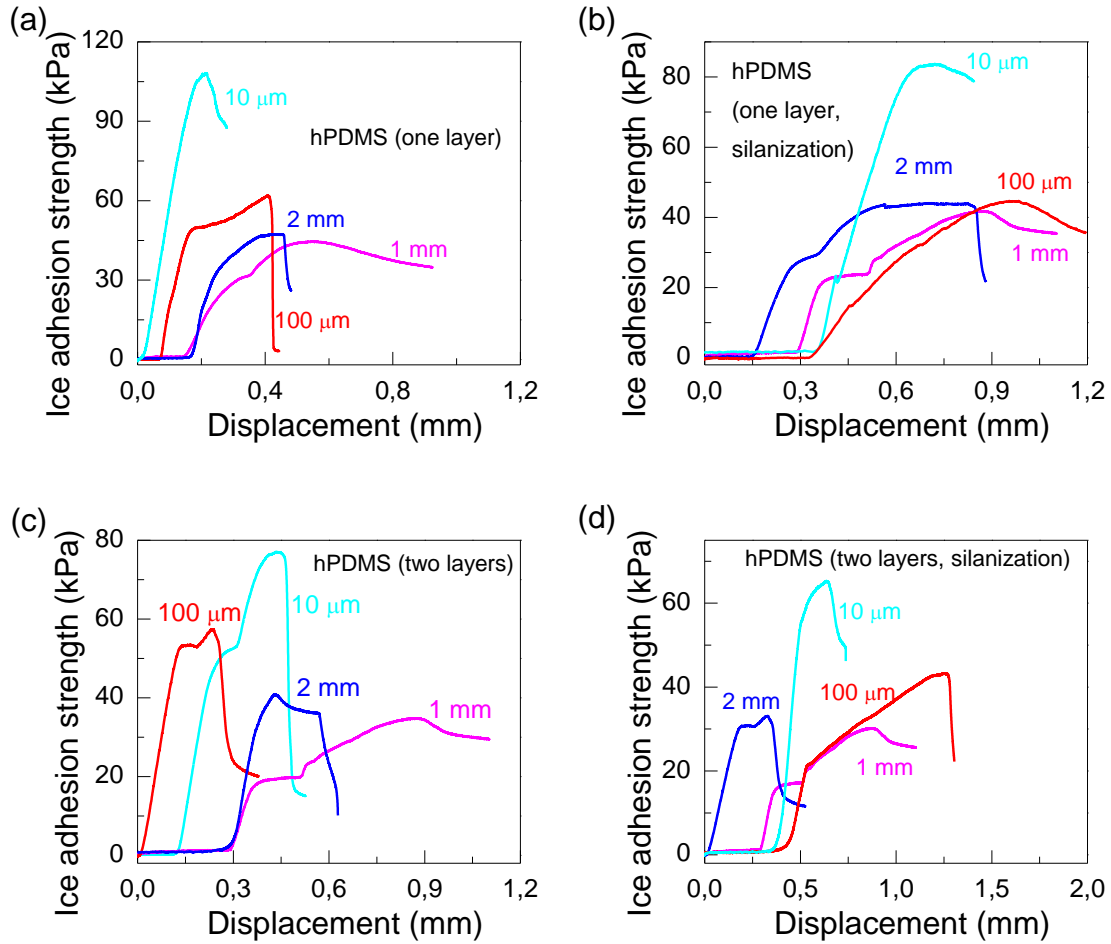


**Fig. S4.** Ice adhesion strength of PDMS thin films at  $-18\text{ }^{\circ}\text{C}$  against displacement. (a) hPDMS with one layer; (b) hPDMS with one layer and silanization; (c) hPDMS with two layers; and (d) hPDMS with two layers and silanization. The single layer thickness is  $30\text{ }\mu\text{m}$ , the curing temperature is  $65\text{ }^{\circ}\text{C}$ , and the weight ratio is 10:1. To realize the design of PDMS with sub-structures as suggested by finite element analysis (**Fig. S1**), a  $67\text{ }\mu\text{m}$  thick thin film of PDMS was coated on glass before preparing targeted PDMS thin films.

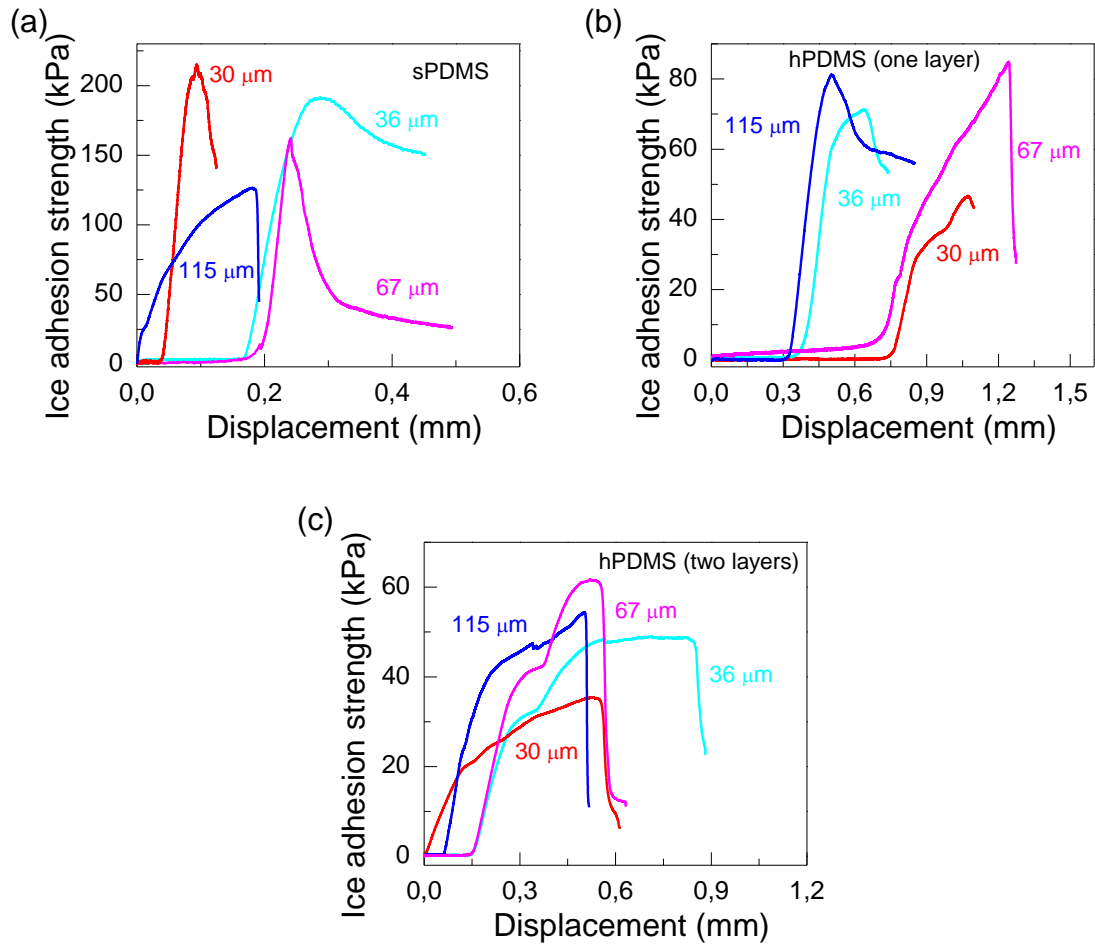


**Fig. S5.** Ice adhesion strength of PDMS thin films at -18 °C against displacement. (a) sPDMS; (b) hPDMS (one layer); and (c) hPDMS (two layers). The diameter of internal holes is 1 mm, the curing temperature is 65 °C, and the weight ratio is 10:1. To realize the design of PDMS with sub-structures as suggested by finite element analysis (**Fig. S1**), a 67 μm thick thin film of PDMS was coated on glass before preparing targeted PDMS thin films.

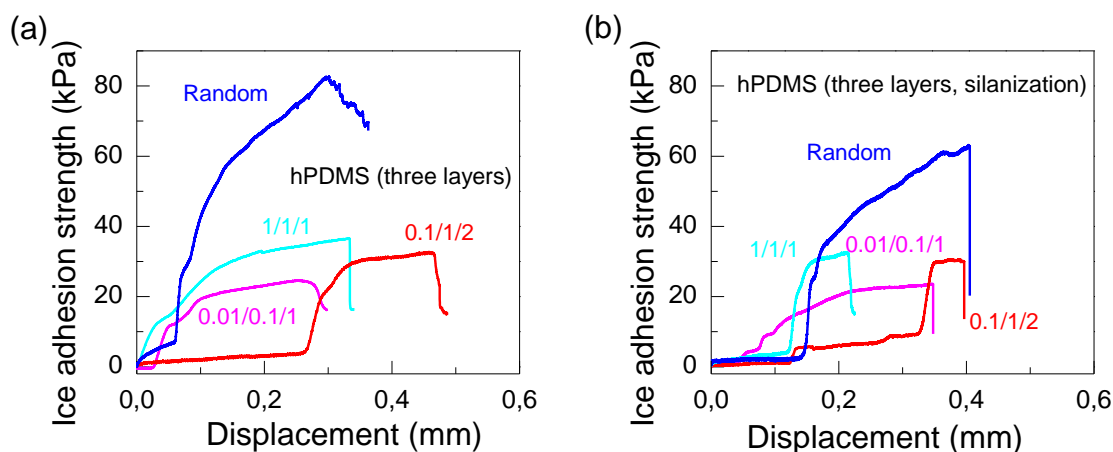


**Fig. S6.** Ice adhesion strength of PDMS thin films at  $-18\text{ }^{\circ}\text{C}$  against displacement. (a) hPDMS (three layers); and (b) hPDMS (three layers, silanization). Three layers with internal holes (bottom-up): 1/1/1, 0.01/0.1/1, 0.1/1/2 in millimeter and random. The single layer thickness is  $30\text{ }\mu\text{m}$ , the diameter of internal holes is 1 mm, the curing temperature is  $65\text{ }^{\circ}\text{C}$ , and the weight ratio is 10:1. As for the random sample, the PDMS agents mixed with  $\text{NH}_4\text{HCO}_3$  powder was coated on glass substrate, cured in a chamber, and then coated with another  $30\text{ }\mu\text{m}$  thick PDMS thin film to make surface smooth. The total thickness of random PDMS sample is the same with other three-layer PDMS thin films. To realize the design of PDMS with sub-structures as suggested by finite element analysis (**Fig. S1**), a  $67\text{ }\mu\text{m}$  thick thin film of PDMS was coated on glass before preparing targeted PDMS thin films.

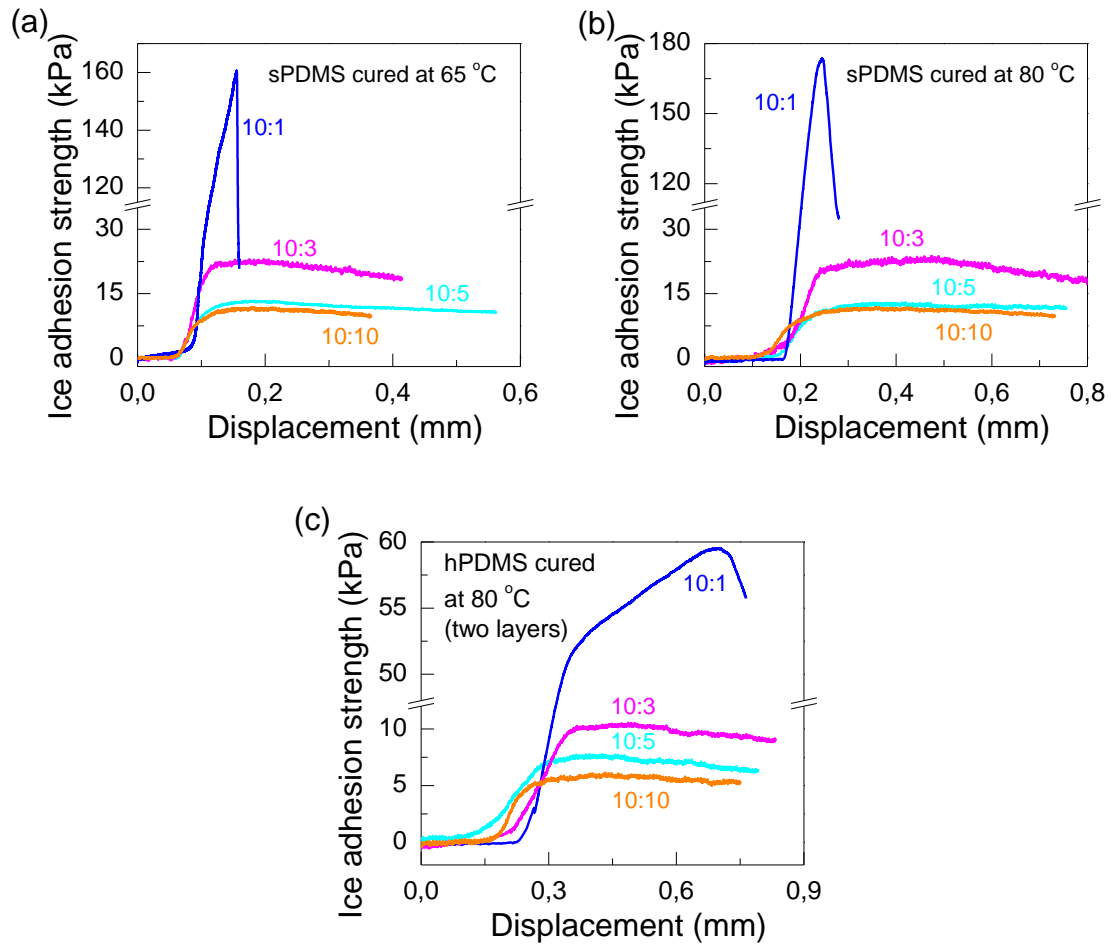


**Fig. S7.** Ice adhesion strength of PDMS thin films at  $-18\text{ }^{\circ}\text{C}$  against displacement. (a) sPDMS cured at  $65\text{ }^{\circ}\text{C}$ ; (b) sPDMS cured at  $80\text{ }^{\circ}\text{C}$ ; and (c) sPDMS cured at  $80\text{ }^{\circ}\text{C}$  (two layers). The single layer thickness is  $67\text{ }\mu\text{m}$ , and the diameter of internal holes is  $1\text{ mm}$ . To realize the design of PDMS with sub-structures as suggested by finite element analysis (**Fig. S1**), a  $67\text{ }\mu\text{m}$  thick thin film of PDMS was coated on glass before preparing targeted PDMS thin films.



**Table S1.** Polydimethylsiloxane (PDMS) surfaces. Four types of PDMS surfaces are prepared in this study, namely sPDMS, hPDMS, pPDMS and hpPDMS. To realize the design of PDMS with sub-structures as suggested by finite element analysis (**Fig. S1**), a 67  $\mu\text{m}$  thick thin film of PDMS is coated on glass. The detailed properties of samples presented in **Fig. 3** are described in the following table.

Samples		Diameter (mm)	Layers	Single layer thickness ( $\mu\text{m}$ )	Weight ratio	Curing Temperature ( $^{\circ}\text{C}$ )	Treatments
Fig. 3a	sPDMS	–	1	30	10:1	65	silanization
	sPDMS	–	1	30	10:1	65	–
	sPDMS	–	1	30	10:1	65	$\text{CF}_4/\text{O}_2$
	hPDMS	0.01	1	30	10:1	65	silanization
	hPDMS	0.01	1	30	10:1	65	–
	hPDMS	0.01	1	30	10:1	65	$\text{CF}_4/\text{O}_2$
	pPDMS	0.01	1	30	10:1	65	silanization
	pPDMS	0.01	1	30	10:1	65	–
	pPDMS	0.01	1	30	10:1	65	$\text{CF}_4/\text{O}_2$
	hpPDMS	0.01	1	30	10:1	65	silanization
	hpPDMS	0.01	1	30	10:1	65	–
hpPDMS	0.01	1	30	10:1	65	$\text{CF}_4/\text{O}_2$	
Fig. 3b	hPDMS	0.01	1	30	10:1	65	–
	hPDMS	0.1	1	30	10:1	65	–
	hPDMS	1	1	30	10:1	65	–
	hPDMS	2	1	30	10:1	65	–
	hPDMS	0.01	1	30	10:1	65	silanization
	hPDMS	0.1	1	30	10:1	65	silanization
	hPDMS	1	1	30	10:1	65	silanization
	hPDMS	2	1	30	10:1	65	silanization
	hPDMS	0.01	2	30	10:1	65	–
	hPDMS	0.1	2	30	10:1	65	–
	hPDMS	1	2	30	10:1	65	–
	hPDMS	2	2	30	10:1	65	–
	hPDMS	0.01	2	30	10:1	65	silanization
	hPDMS	0.1	2	30	10:1	65	silanization
	hPDMS	1	2	30	10:1	65	silanization
hPDMS	2	2	30	10:1	65	silanization	
Fig. 3c	sPDMS	–	1	30	10:1	65	–
	sPDMS	–	1	36	10:1	65	–

	sPDMS	–	1	67	10:1	65	–
	sPDMS	–	1	115	10:1	65	–
	hPDMS	1	1	30	10:1	65	–
	hPDMS	1	1	36	10:1	65	–
	hPDMS	1	1	67	10:1	65	–
	hPDMS	1	1	115	10:1	65	–
	hPDMS	1	2	30	10:1	65	–
	hPDMS	1	2	36	10:1	65	–
	hPDMS	1	2	67	10:1	65	–
	hPDMS	1	2	115	10:1	65	–
Fig. 3d	hPDMS	1/1/1	3	30	10:1	65	–
	hPDMS	0.01/0.1/1	3	30	10:1	65	–
	hPDMS	0.1/1/2	3	30	10:1	65	–
	hPDMS	random	1	90	10:1	65	–
	hPDMS	1/1/1	3	30	10:1	65	silanization
	hPDMS	0.01/0.1/1	3	30	10:1	65	silanization
	hPDMS	0.1/1/2	3	30	10:1	65	silanization
	hPDMS	random	1	90	10:1	65	silanization
Fig. 3e	sPDMS	–	1	67	10:1	65	–
	sPDMS	–	1	67	10:3	65	–
	sPDMS	–	1	67	10:5	65	–
	sPDMS	–	1	67	10:10	65	–
	sPDMS	–	1	67	10:1	80	–
	sPDMS	–	1	67	10:3	80	–
	sPDMS	–	1	67	10:5	80	–
	sPDMS	–	1	67	10:10	80	–
	hPDMS	1	2	67	10:1	80	–
	hPDMS	1	2	67	10:3	80	–
	hPDMS	1	2	67	10:5	80	–
	hPDMS	1	2	67	10:10	80	–

**Table S2.** Summary of the ice adhesion strength of PDMS-based coatings in this study and reported in literature. The ice adhesion strength in this table refers to the shear strength.

	<b>Materials</b>	<b>Temperature (°C)</b>	<b>Ice adhesion strength (kPa)</b>	<b>Ref.</b>
<b>Pure PDMS</b>	PDMS (10:1)	-15	175±13.9	1
	PDMS (10:1)	-10	291±44	2
	PDMS (10:1)	-10	264	3
	PDMS (1:1)	-10	14	3
	PDMS (10:1 to 40:1)	-10 to -40	--	4
	PDMS (10:1)	-10	120-460	5
	<b>hPDMS (10:1)</b>	<b>-18</b>	<b>60</b>	<b>This study</b>
	<b>hPDMS (10:3)</b>	<b>-18</b>	<b>10.6</b>	
	<b>hPDMS (10:5)</b>	<b>-18</b>	<b>7.1</b>	
	<b>hPDMS (10:10)</b>	<b>-18</b>	<b>5.7</b>	
<b>Chemical modified PDMS or PDMS composites</b>	PDMS (1:1)/100-cP SO	-10	<10	3
	Fluorosilane/PDMS	-15	30.0±13.4	6
	Silicon oil/PDMS	-10	40	7
	Lubricant/PDMS	-15	--	8
	PDMSMA-DE/epoxy	-2	97	9
	Nano-silica/PDMS	-5	--	10
	PDMS-b-FPAC	-15	145±13	11
	PDMS organogel	-15	0.4	12
	PDMS organogel	-30	1.7±1.2	13
	PDMS based gel	-20	5.2	14
	5%S17FH/PDMS	-15	105±12	15
	PDMS- <i>b</i> -PFA	-15	187	16

**Table S3.** Roughness on PDMS thin films with different weight ratio, layer thickness, and size of internal holes. To realize the design of PDMS with sub-structures as suggested by finite element analysis (**Fig. S1**), a 67  $\mu\text{m}$  thick thin film of PDMS was coated on glass before preparing targeted PDMS thin films.

<b>Samples</b>	<b>Diameter (mm)</b>	<b>Single layer thickness (<math>\mu\text{m}</math>)</b>	<b>Weight ratio</b>	<b>Roughness Rq (nm)</b>
sPDMS	–	30	10:1	153
	–	30	10:3	127
	–	30	10:5	155
	–	30	10:10	173
hPDMS (two layers)	0.01	30	10:1	218
	0.01	30	10:3	263
	0.01	30	10:5	245
	0.01	30	10:10	238
hPDMS (two layers)	0.01	30	10:1	294
	0.1	30	10:1	315
	1	30	10:1	234
	2	30	10:1	226
hPDMS (two layers)	1	30	10:1	402
	1	36	10:1	349
	1	67	10:1	385
	1	115	10:1	381

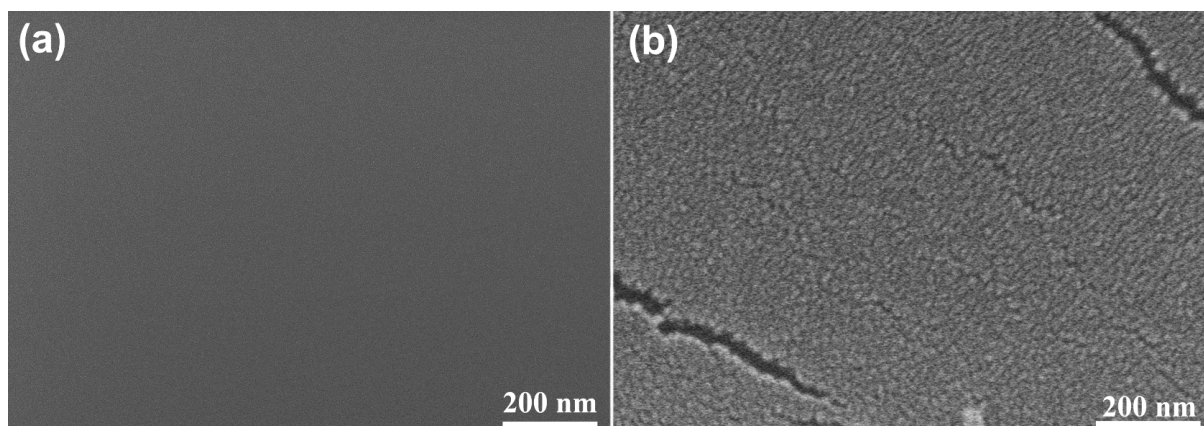


**Fig. S8.** SEM images of PDMS surfaces before (a) and after (b) the  $\text{CF}_4/\text{O}_2$  etching.

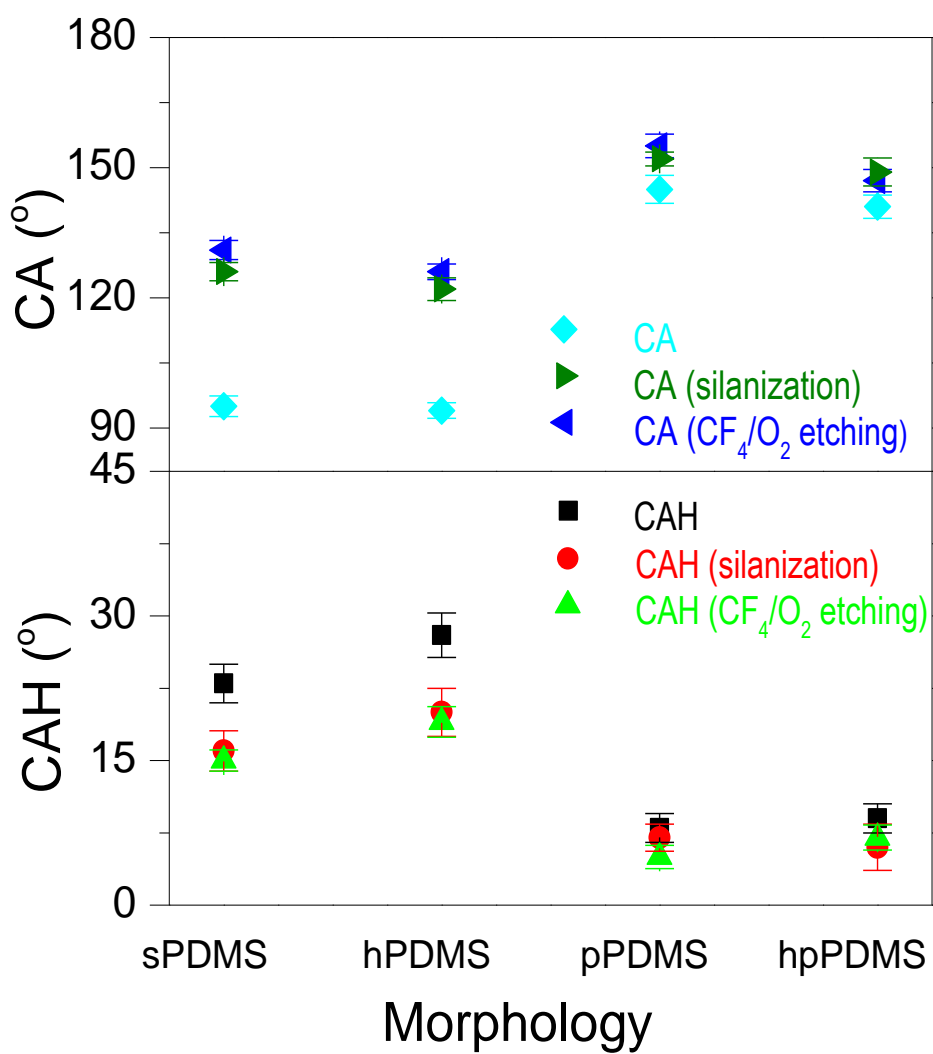
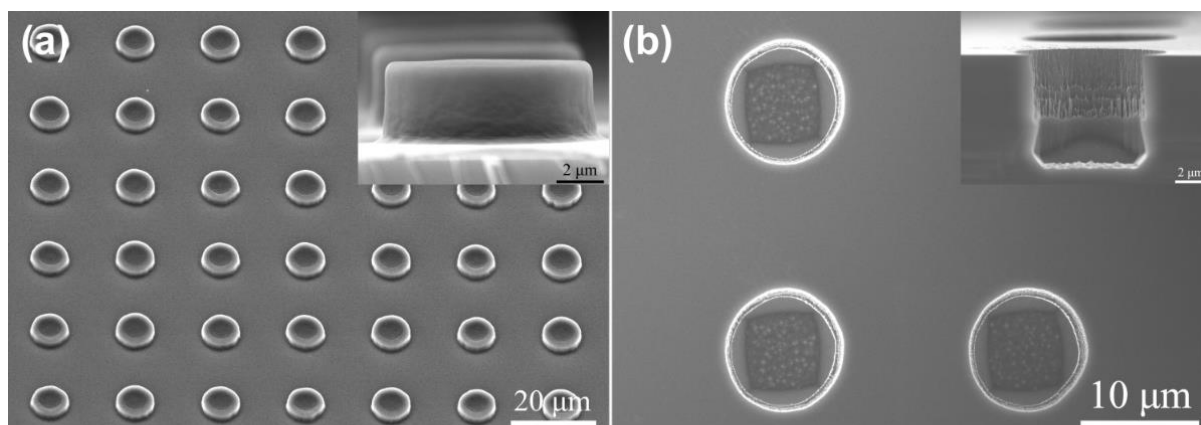
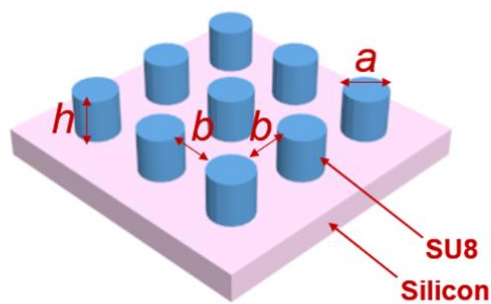


**Fig. S9.** Contact angle (CA) and contact angle hysteresis (CAH) of sPDMS, hPDMS, pPDMS and hpPDMS.



(c)



$$a = b = 10 \mu\text{m (or } 100 \mu\text{m, } 1 \text{ mm, } 2 \text{ mm)}$$

$$h = 3.5 \mu\text{m}$$

**Fig. S10.** Substrates for the preparation of PDMS thin films. (a) Silicon substrate with SU8 pillars; (b) Silicon substrate with holes; (c) Design of SU8 pillars on silicon substrate.

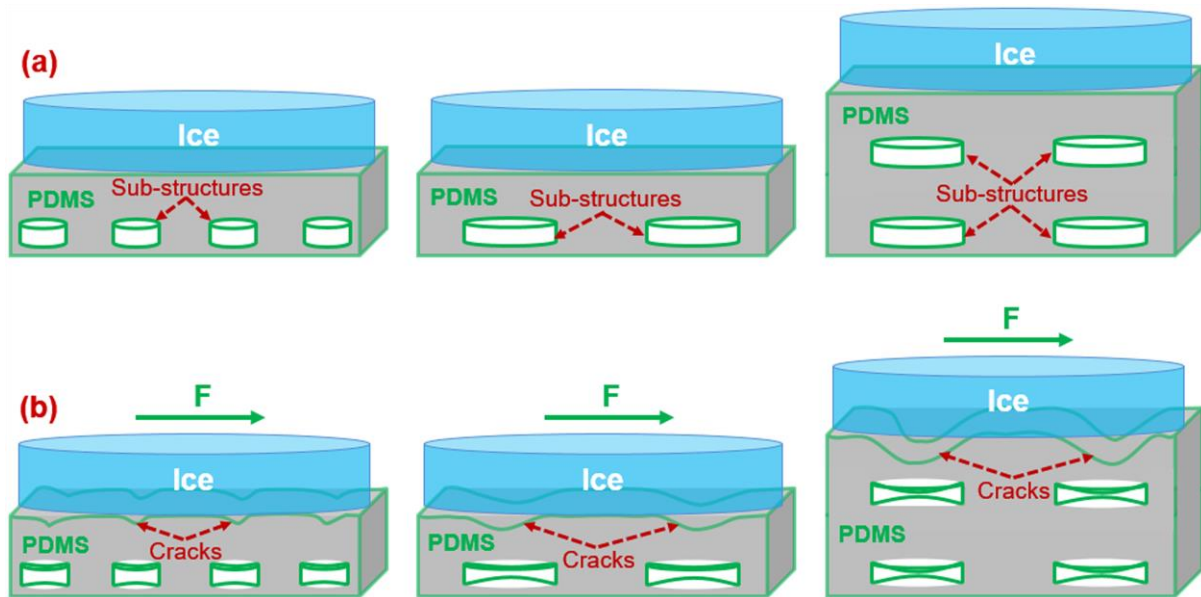


**Fig. S11.** Schematic overview of ice cylinders on PDMS substrates with sub-structures (a) before and (b) during shear loading. The deformations in (a) have been ignored.

Cracks at ice-solid interface induced by MACI mechanism are schematically illustrated in **Fig. S11**. The distance between two adjacent sub-structures is equal to the diameter of internal holes, and the height of internal holes is constant (**Fig. S10**). The maximum possible total length of cracks at ice-solid interface can be considered as the half-length of the solid substrate, which is independent of the size of the internal holes. Of major interest here are the crack openings (driving forces) as shown in **Fig. S11b**. The larger the size of the sub-structures, the larger the crack driving forces at the ice-solid interface, which can dramatically reduce ice adhesion strength.



## REFERENCES

- 1 J. Chen, Z. Luo, Q. Fan, J. Lv and J. Wang, *Small*, 2014, **10**, 4693-4699.
- 2 A. J. Meuler, J. D. Smith, K. K. Varanasi, J. M. Mabry, G. H. McKinley and R. E. Cohen, *ACS Appl. Mater. Interfaces*, 2010, **2**, 3100-3110.
- 3 K. Golovin, S. P. R. Kobaku, D. H. Lee, E. T. DiLoreto, J. M. Mabry and A. Tuteja, *Sci. Adv.*, 2016, **2**, e1501496.
- 4 J. Petit and E. Bonaccorso, *Langmuir*, 2014, **30**, 1160-1168.
- 5 C. Wang, T. Fuller, W. Zhang and K. J. Wynne, *Langmuir*, 2014, **30**, 12819-12826.
- 6 K. K. Varanasi, T. Deng, J. D. Smith, M. Hsu and N. Bhate, *Appl. Phys. Lett.*, 2010, **97**, 234102-234103.
- 7 L. Zhu, J. Xue, Y. Wang, Q. Chen, J. Ding and Q. Wang, *ACS Appl. Mater. Interfaces*, 2013, **5**, 4053-4062.
- 8 X. Yin, Y. Zhang, D. Wang, Z. Liu, Y. Liu, X. Pei, B. Yu and F. Zhou, *Adv. Funct. Mater.*, 2015, **25**, 4237-4245.
- 9 N. Puretskiy, J. Chanda, G. Stoychev, A. Synytska and L. Ionov, *Adv. Mater. Interfaces*, 2015, **2**, 1500124.
- 10 J. Li, Y. Zhao, J. Hu, L. Shu and X. J. Shi, *Adhes. Sci. Technol.*, 2012, **26**, 665-679.
- 11 K.-q. Zhang, J.-z. Cai, X.-h. Li, H. Li, Y.-h. Zhao and X.-y. Yuan, *Chin. J. Polym. Sci.*, 2015, **33**, 153-162.
- 12 C. Urata, G. J. Dunderdale, M. W. England and A. Hozumi, *J. Mater. Chem. A*, 2015, **3**, 12626-12630.
- 13 Y. Wang, X. Yao, J. Chen, Z. He, J. Liu, Q. Li, J. Wang and L. Jiang, *Sci. China Mater.*, 2015, **58**, 559-565.
- 14 D. L. Beemer, W. Wang and A. K. Kota, *J. Mater. Chem. A*, 2016, **4**, 18253-18258.
- 15 K. Zhang, X. Li, Y. Zhao, K. Zhu, Y. Li, C. Tao and X. Yuan, *Prog. Org. Coat.*, 2016, **93**, 87-96.
- 16 H. Li, X. Li, C. Luo, Y. Zhao and X. Yuan, *Thin Solid Films*, 2014, **573**, 67-73.